Catalysis Letters 54 (1998) 41–48 

# Methanol synthesis pathway over $Cu/ZrO_2$ catalysts: a time-resolved DRIFT $^{13}C$-labelling experiment

Enrico E. Ortelli, Johanna M. Weigel and A. Wokaun *

*General Energy Research, Paul Scherrer Institut, CH-5232 Villigen PSI, Switzerland*
*and*
*Department of Chemical Engineering and Industrial Chemistry, Swiss Federal Institute of Technology, ETH Zentrum, CH-8092 Zürich, Switzerland*

Received 4 March 1998; accepted 25 June 1998

To provide additional evidence on the synthesis path of methanol over $Cu/ZrO_2$ catalysts, a three-step *in situ* experiment was performed in a DRIFT cell. $^{13}C$-labelled as well as common $^{12}C$ paraformaldehyde and formic acid were adsorbed and subsequently hydrogenated under reaction conditions (0.5 MPa and 423 K). It was found that methanol was generated exclusively from the $\eta^2$-$H_2CO$ intermediate, not from adsorbed surface formate. Furthermore, the intermediacy of $CO_3^{2-}$ in the reverse/water–gas shift reaction was shown.

**Keywords:** methanol synthesis, $Cu/ZrO_2$, DRIFT, $^{13}C$-labelling experiments

## 1. Introduction

The synthesis of methanol from synthesis gas (CO, $CO_2$, $H_2$) has gained increasing importance in the last decade and is actually one of the most investigated catalytic reactions. Use of methanol in the chemical industries is increasing as a reactant for other organic chemicals such as formaldehyde, MTBE (methyl tertiary-butyl ether), acetic acid, MMA (methyl methacrylate) and DMT (dimethyl terephthalate). Methanol plays also an important role for the storage of $H_2$ as an energy carrier; advantages are that methanol is handled more easily and more conveniently than hydrogen gas. Owing to the fact that $CO_2$ is recognized as the major greenhouse gas, the use of this gas as an alternative feedstock replacing CO in liquid fuel production has received much attention as one promising emission mitigation option.

The formation of methanol proceeds according to the two reaction equilibria:

$$CO + 2H_2 \rightleftharpoons CH_3OH \quad (1)$$

$$CO_2 + 3H_2 \rightleftharpoons CH_3OH + H_2O \quad (2)$$

The use of zirconia-supported copper catalysts is of special interest due to the mechanical and thermal stability, the high specific surface area and semiconducting properties of $ZrO_2$. Although these catalysts have been subject to numerous investigations, the nature of the active sites and of the intermediates continue to be discussed. An issue is the question whether the route to methanol proceeds via formate or other intermediates.

For $ZrO_2$-supported catalysts, He et al. [1,2] have proposed a low temperature mechanism in which formate was hydrogenated to yield a dioxymethylene species, which could react further with hydrogen and desorb as methanol in the presence of water. Abe et al. [3] found for $ZrO_2$ supports experimental evidence for a mechanism proceeding via surface formate and methoxy species. For $Cu/ZrO_2$, Amenomiya [4] concluded that $CO_2$ reacted directly to $CH_3OH$, and that the reverse water–gas shift reaction was taking place in parallel. For the same system, Sun et al. [5] postulated a formate-to-methoxy mechanism when starting from CO as the reactant. Schild et al. [6,7], Köppel et al. [8], Wokaun et al. [9], and Weigel et al. [10] found for $Cu/ZrO_2$-based catalysts that $\pi$-bonded formaldehyde, which is formed in the catalytic reaction of CO and $H_2$, is the key intermediate, and that subsequent reduction yields surface-bound methylate and methanol. The same authors had observed that in a first step surface formates were rapidly formed, in a second step $\eta^2$-$H_2CO$ and adsorbed $H_3CO^-$ were generated simultaneously, and in the last step gas phase $H_3COH$ was detected. More recently, Fisher et al. [11,12] found evidence of a formate → methylenbisoxy → methoxy mechanism for $Cu/ZrO_2/SiO_2$ catalysts.

In this work two intermediates, i.e., $^{13}C$-labelled as well as common formic acid and paraformaldehyde were adsorbed and reduced to investigate the reaction path of methanol synthesis over the $Cu/ZrO_2$ catalyst. Infrared spectra of loaded catalysts were recorded in a DRIFT cell as a function of time on stream.

## 2. Experimental and procedures

### 2.1. Catalyst

The $Cu/ZrO_2$ catalyst used in this study was prepared by coprecipitation of the corresponding metal nitrates at

* To whom correspondence should be addressed.

constant pH and temperature as described elsewhere [13]. It had a composition of $Cu:Zr = 46:54$ at%, and a grain size of 50–150 $\mu$m.

### 2.2. Infrared spectroscopy

Spectra were recorded with a Bruker IFS 55/S EQUINOX Fourier transform infrared spectrometer equipped with a liquid $N_2$ cooled MCT detector. The instrument is equipped with a diffuse reflectance unit and a controlled environmental chamber fitted with NaCl windows (both made by Spectra-Tech). The temperature in the reaction chamber can be regulated with an accuracy of $\pm 1$ K with a home-made temperature control unit using LabView (National Instruments) equipment. The spectra are recorded with a resolution of 4 $cm^{-1}$, with an accumulation of 100–500 interferograms for the time-dependent spectra and 1000 interferograms for background spectra, depending on the respective signal strengths.

### 2.3. Representation of spectra

DRIFT spectra are usually presented in Kubelka–Munk units. In this work we prefer to present the spectra as relative reflectance units ($I/I_0$). This is taking account of the fact that the catalyst of greyish-black color absorbs strongly throughout the mid IR region, and that the reflectance of the loaded catalyst during the reaction is higher than the one of freshly reduced catalyst used as a reference. These properties violate one of the basic assumptions of the Kubelka–Munk theory, i.e., the presence of a non- or weakly absorbing substrate [14,15]. Therefore, the use of relative reflectance units will be more appropriate.

Gaseous products were removed by a continuous stream of the reactant mixture passing over the sample; this results in a reduction of the overlap of bands between surface intermediates and gaseous substances.

### 2.4. Frequencies of labelled substances

The peak position of labelled substances was calculated assuming that isotopically substituted molecules just differ in the respective atomic masses, but have the same bond strengths. Consequently we can write the frequency as

$$\widetilde{\nu} = \frac{1}{2\pi c}\sqrt{\frac{k}{\mu}}, \tag{3}$$

where $k$ is the force constant and $\mu$ is the reduced mass:

$$\mu_{(\mathrm{C-Y})} = \frac{m_{\mathrm{C}} m_{\mathrm{Y}}}{m_{\mathrm{C}} + m_{\mathrm{Y}}}. \tag{4}$$

Here $m_{\mathrm{C}}$ is the mass of the carbon atom and $m_{\mathrm{Y}}$ is the mass of the Y atom bonded to the carbon. From the proportionality (3) we have:

$$\frac{\widetilde{\nu}_{(^{12}\mathrm{C-Y})}}{\widetilde{\nu}_{(^{13}\mathrm{C-Y})}} = \frac{\sqrt{\frac{k}{\mu_{(^{12}\mathrm{C-Y})}}}}{\sqrt{\frac{k}{\mu_{(^{13}\mathrm{C-Y})}}}}. \tag{5}$$

Table 1

| Species | Vibration | Literature ($cm^{-1}$) | This work ($cm^{-1}$) | Figure |
|---|---|---|---|---|
| $\eta^2$-$H_2{}^{12}CO$ | $\nu$(C=O) | 1153 | 1155 | 4 |
| $\eta^2$-$H_2{}^{13}CO$ | $\nu$(C=O) | 1127 | 1130 | 2 |
| $^{12}CH_3OH_{(g)}$ | $\nu$(C–O) | 1034 | 1032 | 4, 5 |
| $^{13}CH_3OH_{(g)}$ | $\nu$(C–O) | 1011 | 1010 | 2, 3 |

Upon substitution of (4) into (5) and evaluation for the C–O and C–H bonds one finds:

$$\widetilde{\nu}_{(^{13}\mathrm{C-O})} = 0.9778\,\widetilde{\nu}_{(^{12}\mathrm{C-O})}, \tag{6}$$

$$\widetilde{\nu}_{(^{13}\mathrm{C-H})} = 0.9970\,\widetilde{\nu}_{(^{12}\mathrm{C-H})}. \tag{7}$$

The shift will be also larger for C–O bonds (>22 $cm^{-1}$) than for C–H bonds (<9 $cm^{-1}$). In table 1 some significant band frequencies are summarized [10–14].

### 2.5. Experimental setup

A gas dosing system equipped with four Brooks 5850E mass flow controllers was coupled to a home-made central control system designed to introduce evaporated liquid and sublimated solid substances into the reaction chamber (figure 1).

Nitrogen (99.999%), hydrogen (99.999%), carbon monoxide (99.998%) and carbon dioxide (99.998%), all from Sauerstoff Lenzburg A.G., were used without further purification. High purity formic acid and paraformaldehyde (both Fluka purum $\geqslant$98%) were used as reference substances; labelled formic acid and paraformaldehyde (both 99%,$^{13}$C; chemical purity $\geqslant$98%) are from Cambridge Isotope Laboratories.

### 2.6. Catalyst preparation

DRIFT spectra are greatly influenced by sample packing [16,17]. To ensure the reproducibility of experiments the catalyst was pressed into the sample cup of the environmental chamber for a constant time of 10 s under a constant pressure of 1 MPa with a home-made sample packing device [18].

The packed catalyst was reduced at 0.1 MPa by heating with a rate of 0.1667 K/s up to 523 K in a nitrogen/hydrogen stream (10 l/h, $H_2:N_2 = 3:1$), and subsequently cooled down to 423 K. Then the background spectrum was recorded.

### 2.7. Experimental procedures

*(a) Adsorption of $^{13}$C-labelled paraformaldehyde and $^{12}$C formic acid followed by reduction:* About 0.2 g of $H_2{}^{13}CO$ was placed in the tube and heated to 403 K. The sublimated substance was flushed with 1 l/h $N_2$ at 0.5 MPa onto the catalyst kept at 423 K. After five minutes 0.1 ml of HCOOH were injected into the 1 l/h $N_2$ flow and also flushed on the catalyst. After five additional

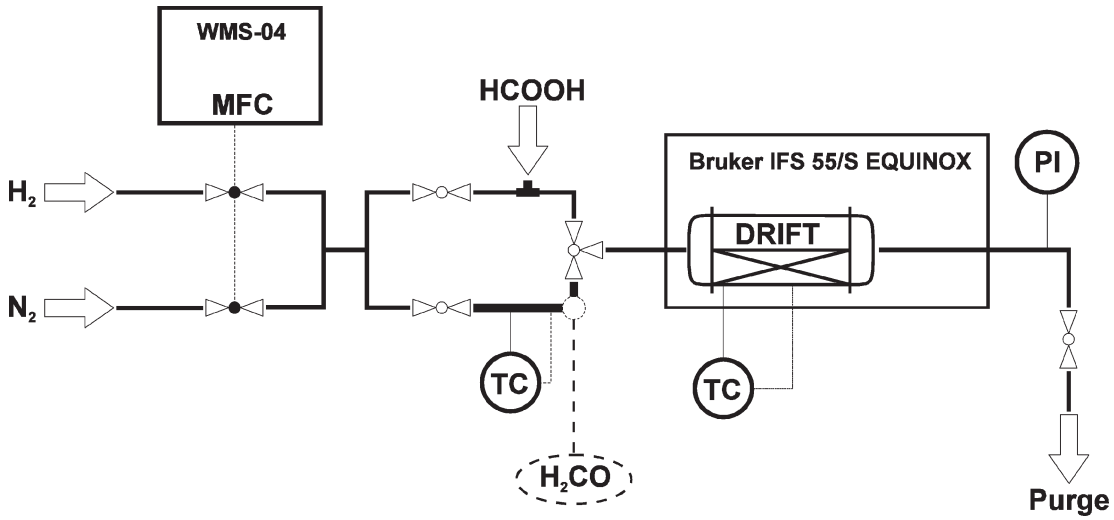


Figure 1. Experimental setup: gas dosing system (MFC: mass flow controllers), the saturation device (upper pathway: evaporator; lower pathway: sublimator) and the DRIFT cell.

minutes the flow was raised to 10 l/h with a composition of $H_2 : N_2 = 3 : 1$.

*(b) Adsorption of $^{13}C$-labelled formic acid and $^{12}C$ paraformaldehyde followed by reduction:* About 0.1 ml of $H^{13}COOH$ was injected into a 1 l/h $N_2$ flow at 0.5 MPa and flushed onto the catalyst kept at 423 K. After five minutes the $N_2$ flow was redirected through the heated tube (403 K) containing 0.2 g of $H_2CO$. Five additional minutes later the flow was raised to 10 l/h with a ratio of $H_2 : N_2 = 3 : 1$ and also passed over the catalyst surface.

## 3. Results and discussion

Detailed assignments of all relevant vibrational bands can be found in the pertinent literature on copper oxides and zirconia-supported catalyst [1–7,9,10,18,19]. In the present communication, we shall focus on a few vibrational features that are informative with regard to the mechanism of methanol synthesis on the specific catalyst investigated.

### *3.1. Adsorption of $H_2{}^{13}CO$ and $H^{12}COOH$*

After switching on the $N_2$ flow containing $^{13}C$-labelled formaldehyde, the spectrum (trace a in figure 2) showed groups of peaks at 1715 $cm^{-1}$ and around 1145 $cm^{-1}$. Both peaks decreased rapidly after switching to the formic acid containing $N_2$-flow (trace d in figure 2). The first above-mentioned band was assigned to $\nu(^{13}C{=}O)$ of gas phase formaldehyde, with contributions from bidentate carbonates (shoulder at 1670 $cm^{-1}$). The second is the result of the contributions of $\nu(^{13}C–O)$ of gas phase paraformaldehyde (1185 $cm^{-1}$), adsorbed paraformaldehyde ($\nu_{as}$, 1070 $cm^{-1}$), $\eta^2$-$H_2{}^{13}CO$ (1130 $cm^{-1}$) (thick arrow in figure 2) and bidentate carbonates ($\nu_{as}$, 1150 $cm^{-1}$ and $\nu_s$, 1220 $cm^{-1}$). $^{13}CO$, from the decomposition of $H_2{}^{13}CO$, showed the corresponding doublet at 2096 $cm^{-1}$; on the other hand $^{13}CO_2$, due to hydrolysis/decomposition of carbonates, appeared at 2282 $cm^{-1}$. Labelled gas phase methanol is immediately present, as evidenced by the $\nu(^{13}C–O)$ band at 1010 $cm^{-1}$ (trace a in figure 2; thin arrow in figures 2 and 3); the R-branch contains a contributions from a methylate band ($\nu(^{13}C–O)$) placed at 1020 $cm^{-1}$. The sharp peak at 915 $cm^{-1}$ has contributions from adsorbed paraformaldehyde ($\nu_s(^{13}C–O)$, 915 $cm^{-1}$) and bidentate carbonates ($\nu_s(^{13}C–O)$, 980 $cm^{-1}$). The band around 2940 $cm^{-1}$ consists of contributions from several substances. Major peaks are the $\nu(^{13}CH_2)$ of adsorbed paraformaldehyde at 2915 $cm^{-1}$; the $\nu_s(^{13}C–H)$ at 2836 $cm^{-1}$ and the shoulder of $\nu_{as}(^{13}C–H)$ at 2970 $cm^{-1}$ of gas phase methanol. Contained within the broad peak are the $\nu(^{13}C–H)$ of methylate ($\nu_{as}$, 2920 $cm^{-1}$ and $\nu_s$, 2820 $cm^{-1}$), of $\eta^2$-$H_2CO$ ($\nu$, 2810 $cm^{-1}$) and of adsorbed paraformaldehyde ($\nu_s$, 2910 $cm^{-1}$). Gas phase water, identified by the typical gas phase multiplet signal around 1620 $cm^{-1}$, will be consumed.

Upon subsequent exposure to an $N_2$/HCOOH flow (traces d, e and f in figure 2), the $^{12}CO_2$-peak (2349 $cm^{-1}$), deriving from decomposition of HCOOH, is growing in intensity together with the $^{13}CO$ (2096 $cm^{-1}$), due to hydrogenation of carbonates (traces d and e in figure 2). The $^{13}CO_2$-peak is also growing in intensity due to hydrolysis/decomposition of carbonates ($*CO_3^{2-} + H_2O \rightleftharpoons CO_2 + 2{*}OH^-$) (traces d and e in figure 2). The bands around 1700 $cm^{-1}$ are no longer detectable. The peak around 1145 $cm^{-1}$ is reduced in intensity, and other peaks are recognizable; i.e., the bidentate carbonates at 1220 $cm^{-1}$ and peaks with contributions from $\eta^2$-$H_2CO$ and adsorbed paraformaldehyde. Before purging with the $H_2/N_2$ flow $^{13}CO$ and $^{13}CO_2$ are strongly decreased (trace f in figure 2).

### *3.2. Hydrogenation of surface species*

Exposing the catalyst that had been loaded as described in the previous section to an $H_2/N_2$ flow, the peaks of methanol, adsorbed paraformaldehyde and $^{13}CO_2$ (1010,

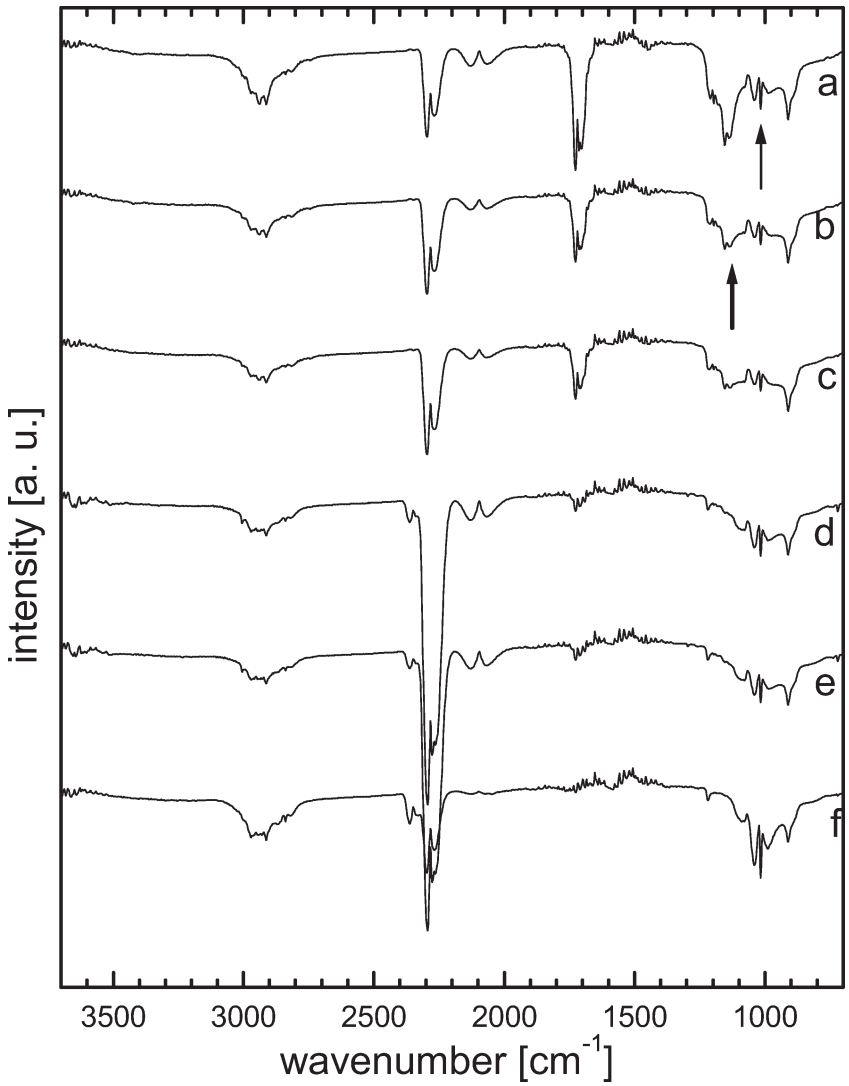


Figure 2. Adsorption of $H_2{}^{13}CO$ for 1, 3 and 5 min (a, b and c), followed by adsorption of $H^{12}COOH$ for 1, 3 and 5 min (d, e and f). The thin and bold arrows designate marker bands of gas phase methanol and adsorbed formaldehyde, as discussed in the text.

2840, 2970 $cm^{-1}$, 915, 1070, 2940 $cm^{-1}$ and 2282 $cm^{-1}$) decrease (traces a, b and c in figure 3). After some minutes gas phase HCOOH peaks grow at 1770 $cm^{-1}$ ($\nu(^{12}C{=}O)$) and at 1120 $cm^{-1}$ ($\nu(^{12}C{-}O)$) together with the bidentate carbonate peaks at 1650 $cm^{-1}$ ($\nu(^{12}C{=}O)$). The peak at 1180 $cm^{-1}$ has contributions from bidentate carbonates ($\nu(^{13}C{-}O)$ at 1220 $cm^{-1}$ and $\nu(^{13}C{-}O)$ at 1070 $cm^{-1}$) (traces d, e and f in figure 3). Continued exposure to the $H_2/N_2$ flow causes a loss in intensity of the methanol bands. The $CO_2$ doublet becomes stronger due to increased formic acid decomposition. Gas phase water is also present, as identified from the typical multiplet of bands around 1620 $cm^{-1}$.

### *3.3. Adsorption of $H^{13}COOH$ and $H_2{}^{12}CO$*

Spectra of a catalyst exposed to a flow of $^{13}C$-labelled formic acid in $N_2$ (traces a and b in figure 4) showed the gas phase formic acid bands at 1730 $cm^{-1}$ ($\nu(^{13}C{=}O)$), at 1095 $cm^{-1}$ ($\nu(^{13}C{-}O)$) and a less intensive band around 2920 $cm^{-1}$ ($\nu(^{13}C{-}H)$). The broad band around 1180 $cm^{-1}$ is caused by a contribution of bidentate carbonates ($\nu(^{12}C{-}O)$ and $\nu(^{13}C{-}O)$); also the two weak peaks at 1415 $cm^{-1}$ and at 1385 $cm^{-1}$ can be assigned to $\nu_{as}$(O–C–O) of $^{13}C$- and $^{12}C$-monodentate carbonates (traces c and d in figure 4). The shoulder at 1525 $cm^{-1}$ that became a sharp peak after a few minutes (traces b and c in figure 4) and the less intensive peak at 1335 $cm^{-1}$ will be assigned to $\nu_{as}(^{13}C{-}O)$ and to $\nu_s(^{13}C{-}O)$, respectively, which together with the $\nu(^{13}C{-}H)$ at 2860 $cm^{-1}$ can be assigned to $^{13}C$-formate (traces a, c and f in figure 4). In the same way the peak at 1570 $cm^{-1}$ (trace a in figure 4) that became a shoulder in later spectra is a contribution of $\nu_{as}(^{12}C{-}O)$ of formates. $^{12}CO_2$ is probably due to the presence of residual air in the injection system.

After switching to the $N_2/^{12}C$-paraformaldehyde gas stream gas phase unlabelled methanol is immediately present (traces e and f in figure 4) as identified by the $\nu$(C–O) signal at 1032 $cm^{-1}$ (thin arrow in figures 4 and 5). Gas phase water is now present. Carbonate peaks at

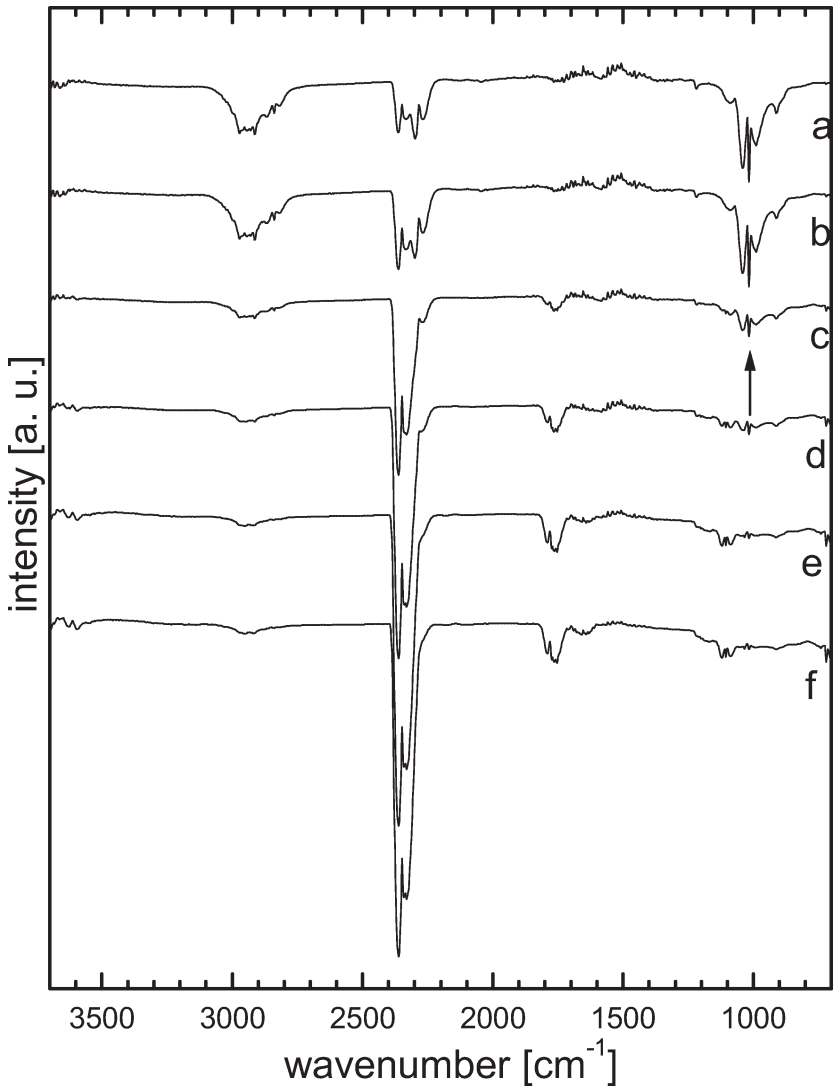


Figure 3. Hydrogenation of species on catalyst surface onto which $H_2{}^{13}CO$ and $H^{12}COOH$ had been previously adsorbed. After switching to $N_2/H_2$, the course of hydrogenation was monitored for 1, 5, 10, 15, 25 and 45 min (a, b, c, d, e and f). The arrow designates the marker band of gas phase methanol.

1415 $cm^{-1}$ and 1385 $cm^{-1}$ are decreasing, due to hydrolysis/decomposition, and simultaneously $^{13}CO_2$ and $^{12}CO_2$ peaks are growing (traces e and f in figure 4). The peak at 1735 $cm^{-1}$ shifts to around 1750 $cm^{-1}$ due to contribution of gas phase formaldehyde ($\nu(^{12}C{=}O)$ at 1755 $cm^{-1}$). Gas phase paraformaldehyde is also present, as visible with the shoulder at 1210 $cm^{-1}$ ($\nu(^{12}C{-}O)$). $\eta^2$-$H_2{}^{12}CO$ (1155 $cm^{-1}$) (thick arrow in figure 4) is formed and finally becomes the predominant peak around 1150 $cm^{-1}$. The weak peak at 1650 $cm^{-1}$ will be assigned to the $\nu(C{=}O)$ of bidentate carbonates. The peak around 2950 $cm^{-1}$ contains contributions from $\nu(C{-}H)$ of paraformaldehyde (2915 $cm^{-1}$) and methanol (2975 $cm^{-1}$), the peak at 2820 $cm^{-1}$ will be assigned to adsorbed formaldehyde.

### *3.4. Hydrogenation of surface species*

Exposing the surface of the catalyst that had been loaded as described in section 3.3 to an $H_2/N_2$ flow effects a rise of the gas phase $^{12}C$-methanol peak at 1032 $cm^{-1}$, and a little the rise of the $^{12}CO$ peak at 2144 $cm^{-1}$, due to hydrogenation of carbonates and to $H_2CO$ decomposition (traces b, c and d in figure 5). After 10 min a little decrease of the 1525 $cm^{-1}$ peak indicated that $^{13}C$-formates are reduced (traces a and d in figure 4). A small amount of monodentate carbonates ($\nu_{as}(O{-}C{-}O)$ at 1415 $cm^{-1}$) is formed on the surface. Gas phase water is always present.

## 4. Conclusions

In the first experiment described, adsorption of $^{13}C$-labelled paraformaldehyde led to the formation of adsorbed paraformaldehyde and surface-bound formaldehyde ($\eta^2$-$H_2CO$), which was consumed after switching on the $H_2/N_2$ flow. Carbon monoxide ($^{13}CO$), which is generated by $H_2CO$ decomposition, led to surface carbonates. *In the gas phase $^{13}C$-labelled methanol was clearly detected with its*

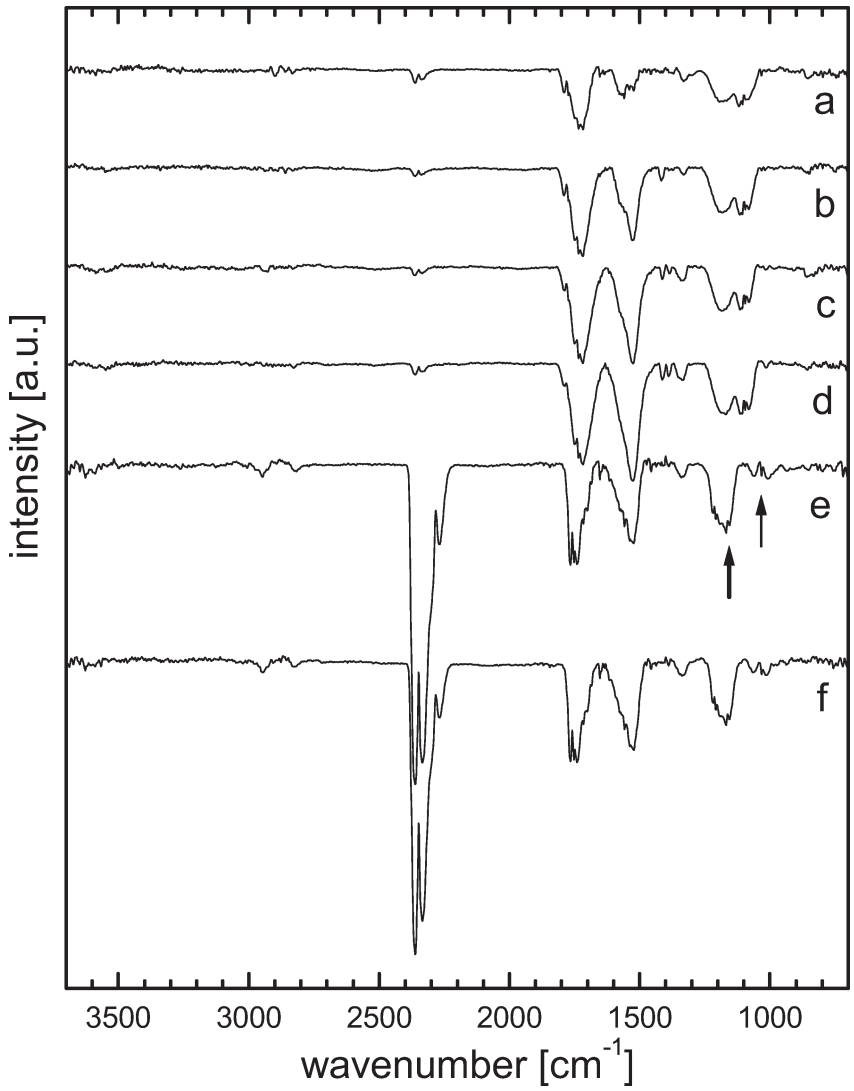


Figure 4. Adsorption of $H^{13}COOH$ for 1, 3 and 5 min (a, b and c), followed by adsorption of $H_2{}^{12}CO$ for 1, 3 and 5 min (d, e and f). The thin and bold arrows designate marker bands of gas phase methanol and adsorbed formaldehyde, as discussed in the text.

*$\nu(^{13}C–O)$ signal at 1010 $cm^{-1}$*. Subsequent adsorption of $^{12}$C-formic acid led to to decomposition of HCOOH into $H_2$ and $CO_2$ and consequently hydrogenation of parts of carbonates into $^{13}$CO. Hydrogenation of the surface led to a reduction of all present paraformaldehyde species. Part of the carbonates present were hydrolyzed/decomposed to release $^{13}CO_2$; besides, additional non-reactive carbonates were formed. *Labelled methanol* was always present. No surface-bound $^{13}$CO, nor labelled surface formates were observed even after long exposure and hydrogenation time. No appreciable change in the concentration of surface hydroxyl groups was observed.

In the second experiment described, the adsorption of $^{13}$C-labelled formic acid generated surface carbonates and surface formates. No methanol or methylate signals were observed. Subsequently, *adsorption of $H_2{}^{12}CO$ rapidly led to a formation of gas phase unlabelled $CH_3OH$ ($\nu(^{12}C–O)$ band at 1032 $cm^{-1}$)*, and to a hydrolysis/decomposition of carbonates (see the rising of the $^{13}CO_2$ band). No labelled adsorbed paraformaldehyde was observed. Under reducing atmosphere, a rise of $^{12}$CO due to decomposition of $H_2{}^{12}CO$ together with a small decrease of formates and formation of carbonates were observed. No adsorbed CO was observed. No appreciable production or decrease of surface hydroxyl groups was observed.

### 4.1. Water–gas shift reaction

The observations suggest that CO and $CO_2$ can be interconverted via surface carbonates, according to the equilibria:

$$CO + 2{*}OH^- \rightleftharpoons {*}CO_3^{2-} + H_2 + {*} \quad (8)$$

$${*}CO_3^{2-} \rightleftharpoons {*}O^{2-} + CO_2 \quad (9)$$

$${*} + {*}O^{2-} + H_2O \rightleftharpoons 2{*}OH^- \quad (10)$$

where $*$ designates an adsorption site. This scheme is supported by the following observations. In the first experiment (figure 2) the $^{13}$C source is the $^{13}$CO. $^{13}CO_2$ and $^{13}$C-

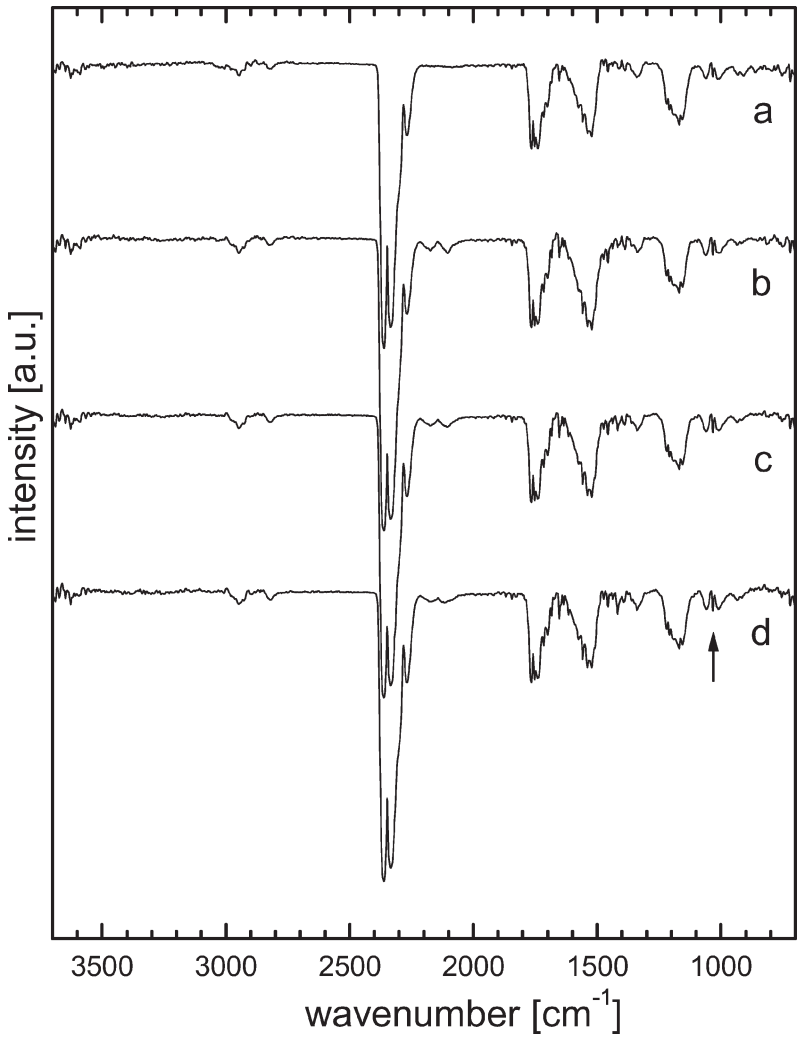


Figure 5. Hydrogenation of species on catalyst surface onto which $H^{13}COOH$ and $H_2{}^{12}CO$ had been previously adsorbed. After switching to $N_2/H_2$, the course of hydrogenation was monitored for 1, 3, 5 and 10 min (a, b, c and d).

carbonates must be generated from this source. In the presence of water (consumption of gas phase water) carbonates will be hydrolyzed/decomposed and $^{13}CO_2$ will be formed. During the hydrogenation step some $^{12}CO_2$ is present and a little gas phase water is consumed (traces e and f in figure 3), as the system is close to equilibrium. In the second experiment (figure 4) we find that $^{12}$C-carbonates are generated from $^{12}CO_2$. During the hydrogenation step (figure 5) we find that $^{12}$C-carbonates are reduced and some $^{12}$CO together with gas phase water is produced. This result is also in agreement with previous observations [10–13].

### *4.2. Methanol formation*

Useful information is provided in addition on the methanol synthesis route. The observations suggest that surface-bound formaldehyde is the key intermediate according to the equilibria:

$$*\eta\text{-}H_2CO + *OH^- \overset{H_2}{\rightleftharpoons} * H_3CO^- + *OH_2 \quad (11)$$

$$*H_3CO^- + *OH_2 \rightleftharpoons * + *OH^- + H_3COH \quad (12)$$

This is supported by the fact that it was not possible to find methylate or methanol without the presence of $\eta^2$-$H_2CO$ on the surface (figures 2, 4 and 5), and that even after long exposure to a hydrogen atmosphere no surface formate species were reduced to methanol (figures 3 and 5), i.e., no methanol of same isotope as formate was observed. Most importantly, the isotope of carbon atom of methanol and the one of adsorbed formaldehyde were always of the same type (figures 2, 4 and 5). It was never possible to observe CO bound to the surface. We conclude that the C-source of the methanol carbon was always the formaldehyde carbon respectively the $\eta^2$-$H_2CO$ carbon. This result confirms the mechanism proposed from previous observations [10–14,20].

**Acknowledgement**

We are grateful to Professor Dr. A. Baiker of ETH Zürich for providing the catalyst. Thanks are due to Dr. J. Wambach and M. Meli for suggestions on the manuscript.

## References

[1] M.-Y. He and J.G. Ekerdt, J. Catal. 87 (1984) 238.
[2] M.-Y. He, J.M. White and J.G. Ekerdt, J. Mol. Catal. 30 (1985) 415.
[3] H. Abe, K. Maruya, K. Domen and T. Onishi, Chem. Lett. (1984) 1875.
[4] Y. Amenomiya, Appl. Catal. 30 (1987) 57.
[5] Y. Sun and P.A. Sermon, J. Chem. Soc. Chem. Commun. (1993) 1242.
[6] C. Schild, A. Wokaun and A. Baiker, J. Mol. Catal. 63 (1990) 223.
[7] C. Schild, A. Wokaun and A. Baiker, Fres. J. Anal. Chem. 341 (1991) 395.
[8] R.A. Köppel, A. Baiker, C. Schild and A. Wokaun, J. Chem. Soc. Faraday Trans. 87 (1991) 2821.
[9] A. Wokaun, J. Weigel, M. Kilo and A. Baiker, Fres. J. Anal. Chem. 349 (1994) 71.
[10] J. Weigel, C. Fröhlich, A. Baiker and A. Wokaun, Appl. Catal. 140 (1996) 29.
[11] I. Fisher, H.-C. Woo and A.T. Bell, Catal. Lett. 44 (1997) 11.
[12] I. Fisher ant A.T. Bell, J. Catal. 172 (1997) 222.
[13] C. Fröhlich, R.A. Köppel, A. Baiker, M. Kilo and A. Wokaun, Appl. Catal. A 106 (1993) 275.
[14] P. Kubelka and F. Munk, Z. Tech. Phys. 11(a) (1931) 593.
[15] P. Kubelka, J. Opt. Soc. Am. 38 (1948) 448.
[16] S.A. Yeboah, S.-H. Wang and P.R. Griffths, Appl. Spec. 38(2) (1984) 259.
[17] Z. Krivácsy and J. Hlavay, J. Spec. Acta 50A (1994) 49.
[18] C. Schild, A. Wokaun and A. Baiker, J. Mol. Catal. 63 (1990) 243.
[19] G.J. Millar, C.H. Rochester and K.C. Waugh, J. Chem. Soc. Faraday Trans. 88 (1992) 2257.
[20] J.M. Weigel, Ph.D. thesis, ETH, Zürich (1996).